PERSISTENT SCATTERER INTERFEROMETRY BASED ON TERRASAR-X IMAGERY: THE BARCELONA TEST AREA

M. Crosetto[a,*], O. Monserrat[a], M. Cuevas[a], B. Crippa[b]

[a] Institute of Geomatics, Av. del Canal Olímpic, s/n, Castelldefels, E-08860, Spain
michele.crosetto@ideg.es, oriol.monserrat@ideg.es, maria.cuevas@ideg.es
[b] Department of Earth Sciences, University of Milan, Via Cicognara 7, 20129 Milan, Italy - bruno.crippa@unimi.it

Commission VII, WG VII/2

KEY WORDS: Remote Sensing, Satellite, Detection, Deformation, Geocoding.

ABSTRACT:

The aim of this paper is deformation monitoring over urban areas using Persistent Scatterer Interferometry (PSI) and Very High Resolution (VHR) X-band SAR imagery. Since the launch of TerraSAR-X and the first COSMO-SkyMed satellite (both were launched in June 2007), the VHR X-band data has grown in importance as source of PSI. This is due to the remarkable increase of the data acquisition capability (for instance, the COSMO-SkyMed constellation consists of three SAR satellites in mid 2010), the progressive loss of key sources of SAR images, as ASAR-Envisat and ERS-2, and the promising technical characteristics of the X-band. This paper illustrates some of the main results of the PSI analysis derived from VHR X-band data. The analysis was carried out over a stack of SAR images captured by the TerraSAR-X sensor and covering the metropolitan area of Barcelona (Spain). This work is the first experience of the authors with PSI analysis of the X-band, which is based on a rich set of 28 StripMap images. These images were processed and analysed using the PSI in-house experimental software chain of the Institute of Geomatics. A description of the Barcelona dataset and the main outcomes of the PSI analysis is given. These outcomes reflect a preliminary assessment of the improvement which can be achieved by VHR X-band PSI, mainly in terms of deformation monitoring capability.

1. INTRODUCTION

This paper describes a technique for deformation monitoring over urban areas based on Persistent Scatterer Interferometry (PSI) and very high resolution (VHR) X-band Synthetic Aperture Radar (SAR) images, captured by the TerraSAR-X sensor. In particular, it summarizes the experience of the authors in the analysis of a test area: the metropolitan area of Barcelona (Spain).

PSI is a radar-based remote-sensing technique to measure and monitor land deformation (see Rosen et al., 2000; Crosetto et al., 2005). PSI represents the most advanced category of DInSAR techniques. Different PSI approaches have been proposed in the last decade (see Ferretti et al., 2001; Berardino et al., 2002; Colesanti et al., 2003; Mora et al., 2003; Lanari et al., 2004; Hooper et al., 2004; Kampes and Hanssen, 2004; Crosetto et al., 2005; Pepe et al., 2005; Crosetto et al., 2008).

The availability of SAR data acquired by space-borne sensors represents a key issue for the successful use of PSI. In particular, image acquisition continuity over large periods of time plays a fundamental role in PSI. Note that the data must be acquired by the same sensor or compatible sensors, as in the case of ERS-1 and ERS-2. The first satellite that allowed demonstrating the potentialities of the PS technique was ERS-1. This satellite has been operative for 10 years and, more importantly, together with its almost exact replica ERS-2, has provided a valuable historical archive of interferometric SAR data. ERS satellites have provided global spatial coverage over a time period of 19 years, with the first images dating back to summer 1991. There are hundreds of high level scientific publications that demonstrate the success of the ERS mission. Radarsat-1 and ASAR-Envisat have also been particularly important PSI data sources. The latest Differential Interferometric SAR (DInSAR) results based on data acquired by the ERS and Envisat satellites can be found at http://eopi.esa.int/

A new generation of sensors has been launched in the last few years, including the C-band Radarsat-2 (launched in December 2007 by the Canadian Space Agency), the X-band TerraSAR-X (launched in June 2007 by a joint venture carried out under a public-private-partnership between the German Aerospace Centre, DLR, and EADS Astrium GmbH; the exclusive commercial exploitation rights are held by Infoterra GmbH), and the X-band COSMO-SkyMed (COnstellation of small Satellites for the Mediterranean basin Observation, conducted by the Italian Space Agency, ASI; the current constellation includes three satellites).

The last two systems, TerraSAR-X and COSMO-SkyMed are particularly promising due to their very high spatial resolution imaging capabilities and the use of the X-band. One of the key tasks of the PSI research teams spread all over the world is to study the performance of these two very promising types of SAR data. The goal of this paper is to describe the first experience of the authors in the PSI analysis based on a rich set of TerraSAR-X images. These images were processed using the PSI in-house experimental software chain of the Institute of Geomatics. This paper describes a dataset covering the metropolitan area of Barcelona and the main outcomes of the preliminary PSI analysis.

* Corresponding author.

Figure 1. Metropolitan area of Barcelona: SAR amplitude superimposed over Google Earth. The area covers 45 by 45 km approx.

2. THE BARCELONA DATASET

The VHR X-band SAR dataset analysed in this paper is composed of 28 StripMap images acquired by the sensor onboard the satellite TerraSAR-X. This dataset is an interferometric stack of images covering the same area, i.e. they are suitable to perform a PSI analysis. The spatial coverage of the images is shown in Figure 1, while their temporal distribution, which starts in December 2007 and ends in November 2009, can be found in Table 1. Six of the 28 images were acquired for the Project Nº. LAN0634, "Evaluation of DEM derived from TerraSAR-X data", of the TerraSAR-X Science Service Program. Some preliminary results of a subset of 13 SAR images are described in Crosetto et al. (2010).The images used in this work cover approximately 30 by 50 km, with a pixel footprint of about 1.9 by 1.6 m. The images were acquired with an off-nadir angle of 35.5º. The perpendicular baselines of the interferograms based on these images (i.e. the component of the vector that connects the two satellite positions during image acquisition, measured in the direction perpendicular to the SAR line-of-sight) are approximately in the range of -275 m to 500 m.

In the next sections, the following aspects are analysed: (i) the spatial sampling, (ii) the so-called residual topographic error and the PSI geocoding and (iii) the average displacement rates and the deformation time series.

Acquisition dates	
20071230	20080908
20080110	20081102
20080121	20081216
20080212	20090118
20080223	20090129
20080305	20090220
20080316	20090314
20080429	20090416
20080521	20090530
20080612	20090713
20080623	20090815
20080704	20090917
20080715	20091020
20080817	20091122

Table 1. Temporal distribution of the 28 images considered in this study The temporal coverage is approximately two years: from December 2007 to November 2009.

Figure 2. Example of the sampling capability of TerraSAR-X StripMap imagery. A photo of the Agbar tower, an emblematic 144 m height skyscraper of Barcelona, is shown in the left image. The mean SAR amplitude image over the same tower is shown in the right image. In this case, the mean amplitude image was obtained using 20 co-registered images. One sample every 0.75 m along the vertical direction can be obtained thanks to the resolution in range of these images (0.9094 m).

3. SPATIAL SAMPLING

As mentioned above, the major advantage of the X-band imagery captured by the sensors onboard the TerraSAR-X and COSMO-SkyMed satellites is its high spatial resolution (see Adam et al., 2008). Figure 1 shows an illustrative example of a skyscraper: a very dense sampling of vertical facades is provided by TerraSAR-X. However, it is worth emphasising that the actual PSI spatial sampling capability, and hence the PSI deformation measurement capability, is usually much lower than the resolution of the original SAR imagery. In fact, PSI deformation measurements can only be achieved for the points where PSI phases maintain good quality over time. An example of PSI sampling density is shown in Figure 3. It is evident that many of the original SAR pixels cannot be exploited to estimate deformation in this case (e.g. see the central part of the image where no measurements were obtained). However, a very dense set of deformation measurement points can be obtained where the PSI phase maintains good quality.

4. PSI GEOCODING

An interesting aspect of the analysis of the TerraSAR-X data described in this work is the accurate PSI geocoding capability, which is a fundamental step to correctly interpret and exploit the PSI results. A key step to achieve this geocoding is the estimation, for each PSI measured point, of the so-called residual topographic error (see Crosetto et al., 2010), which is one of the main PSI products.

An example of PSI geocoding is shown in Figure 4, which shows the residual topographic error estimated over the Camp Nou stadium. Note that the optical image used as background (to show the geocoding quality) shows the typical geometric distortions of the standard ortho-images (i.e. it is not a so-called true ortho-image). Another interesting example of PSI geocoding is shown in Figure 5.

5. DEFORMATION ANALYSIS

The estimation of the deformation of the area at hand and during the observed period is the main outcome of the PSI analysis. It usually yields two main products: (i) the average displacement rates over the observed period, and (ii) the time series of the deformation. In this paper we only consider the first product. An example of average displacement rates is shown in Figure 3. The most important characteristic of this example is the high density of measurements achieved through PSI analysis. This example is complemented by another deformation measurement result, shown in Figure 6, not obtained by means of a PSI analysis. With a simple standard interferometric analysis based on two images, interesting deformation phenomena may be found. This result, achieved with just two images, is important, especially considering the high commercial price of the TerraSAR-X images.

Even though the results shown in this paper are rather preliminary, they are very promising. Additional work is needed to make a comprehensive assessment of PSI TerraSAR-X: defining the key achievements in terms of new applications, their advantages and limitations, their monitoring performances with respect to costs, etc.

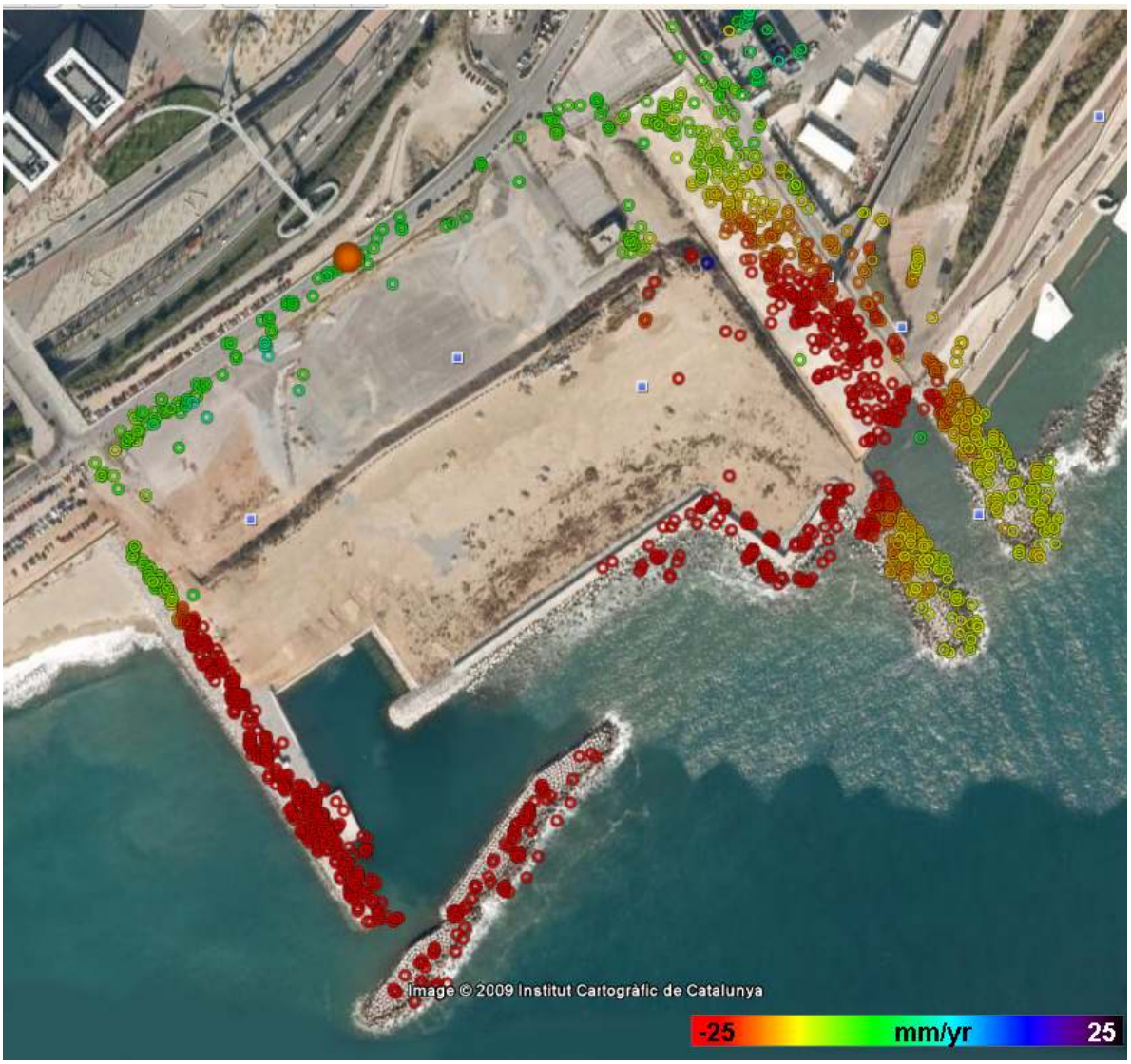

Figure 3. Geocoded deformation velocity map superimposed over a Google Earth image. The red colours represent subsidence areas. The map covers the construction area of the zoo of Barcelona. Significant portions of this area suffer subsidence up to -25 mm/yr. The high sampling density achieved over some of the infrastructures can be observed.

ACKNOWLEDGEMENTS

This work has been mainly funded by the Spanish Ministry of Science and Innovation through the project LIRA (ref. LIRA_MEP_2009_1-0). Six of the 28 images come from the Project Nº. LAN0634, "Evaluation of DEM derived from TerraSAR-X data", of the TerraSAR-X Science Service Program.

REFERENCES

Adam, N., Eineder, M., Yague-Martinez, N., Bamler, R., 2008. High Resolution Interferometric Stacking with TerraSAR-X. In: *Proceedings of IGARSS 2008*, Boston, USA.

Berardino, P., Fornaro, G., Lanari, R., Sansosti, E., 2002. A new algorithm for surface deformation monitoring based on small baseline differential SAR interferograms. *IEEE Transactions on Geoscience and Remote Sensing*, 40(11), pp. 2375-2383.

Colesanti, C., Ferretti, A., Novali, F., Prati, C., Rocca, F., 2003a. SAR monitoring of progressive and seasonal ground deformation using the Permanent Scatterers Technique. *IEEE Transactions on Geoscience and Remote Sensing*, 41(7), pp. 1685-1701.

Crosetto, M., Crippa, B., Biescas, E., Monserrat, O., Agudo, M., Fernández, P., 2005. Land deformation monitoring using SAR interferometry: state-of-the-art. *Photogrammetr. Fernerkundung Geoinformation*, 6, pp. 497-510.

Crosetto. M., Biescas, E., Duro, J., Closa, J., Arnaud, A., 2008. Quality assessment of advanced interferometric products based on time series of ERS and Envisat SAR data. *Photogrammetric Engineering and Remote Sensing*, 74(4).

Crosetto, M., Monserrat, O., Iglesias, R., Crippa, B., 2010. Persistent Scatterer Interferometry: potential, limits and initial C- and X-band comparison. *Photogrammetric Engineering and Remote Sensing*, Special Issue (in press).

(the reference list continues in the last page of the paper)

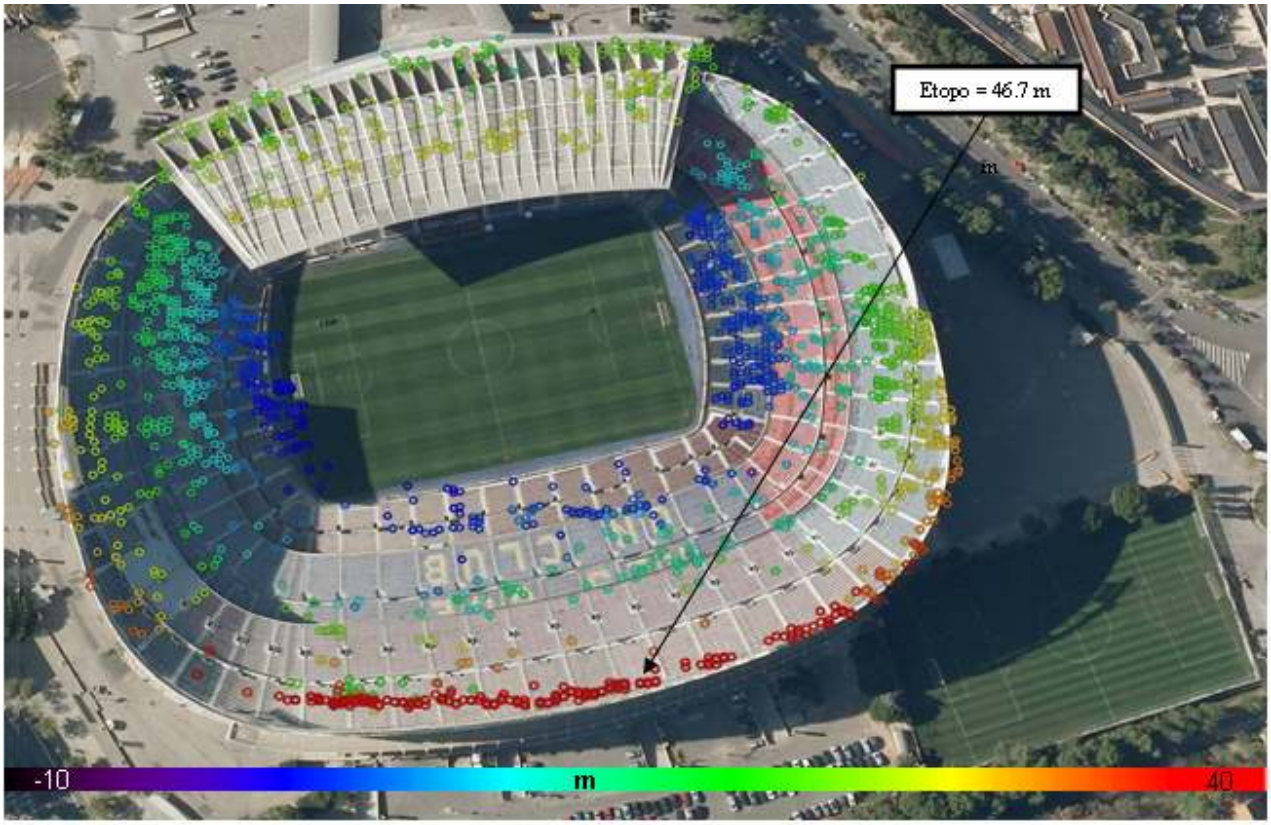

Figure 4. Example of PSI geocoding over the Camp Nou stadium. This is a geocoded map of the residual topographic error estimated for each PSI-measured point, which is superimposed over a Google Earth optical image. The different colours represent residual topographic error, which roughly corresponds to the elevation with respect to a digital terrain model of the area from the Cartographic Institute of Catalonia.

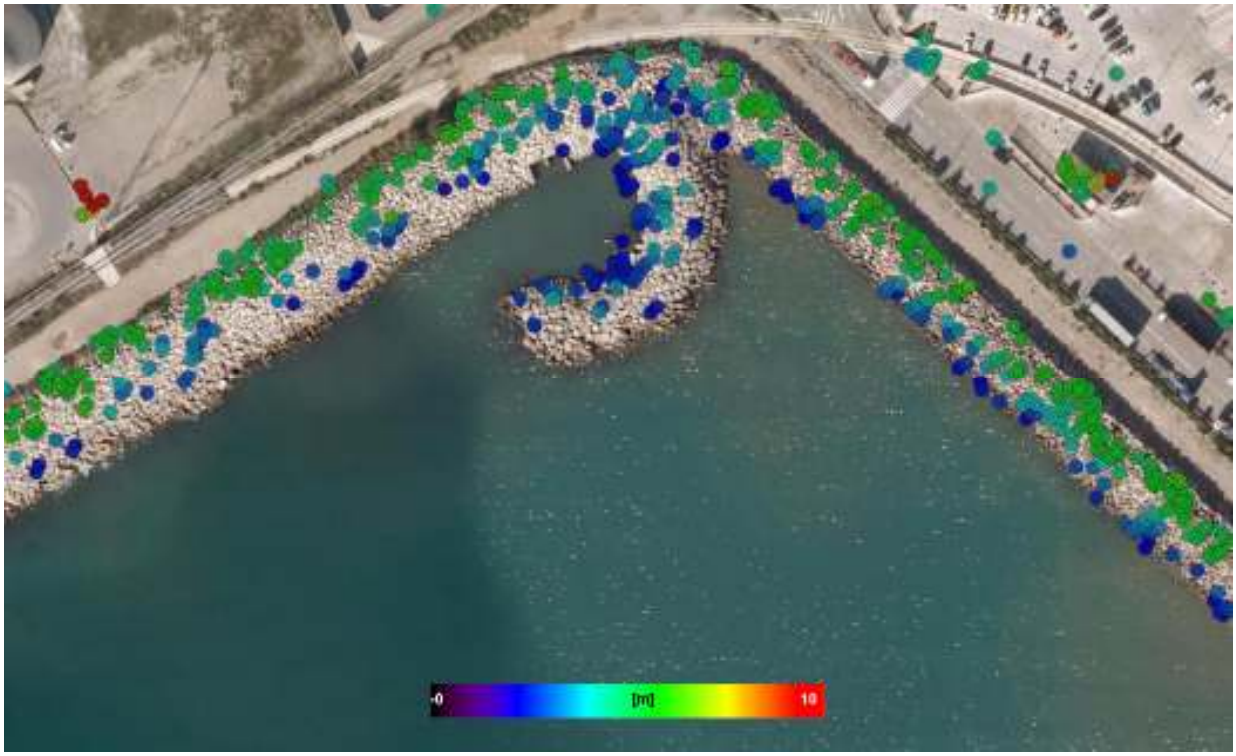

Figure 5. Example of PSI geocoding over a portion of the Port of Barcelona. In this case, the good geocoding accuracy of the PSI results can be observed. The colour of the measured points represents the residual topographic error, which roughly corresponds to the elevation with respect to a digital terrain model of the area from the Cartographic Institute of Catalonia, as in Figure 4.

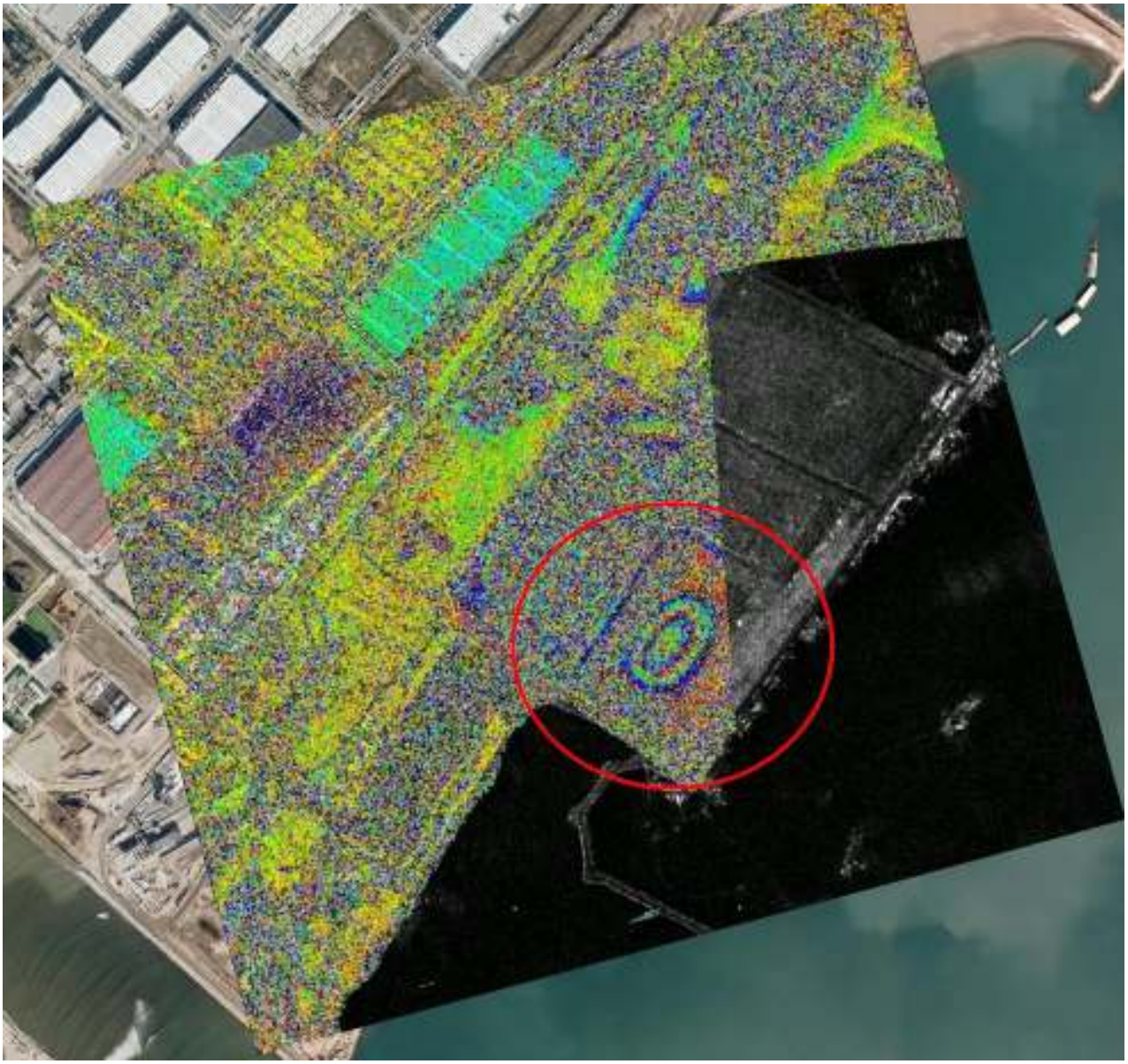

Figure 6. Example of deformation measurement based on a single interferogram. The image is a wrapped interferogram with a temporal baseline of 11 days, which is superimposed over a SAR amplitude image. Google Earth images are used as background. The red circle shows an ellipse that includes two phase fringes. The maximum deformation is approximately 3 cm. It is therefore a relatively fast deformation of 3 cm in 11 days. This result, achieved with just two images, is important especially if the high commercial price of the TerraSAR-X images is considered.

Ferretti, A,, Prati, C., Rocca, F., 2001. Permanent scatterers in SAR interferometry. *IEEE Transactions on Geoscience and Remote Sensing,* 39(1), pp. 8-20.

Hooper, A., Zebker, H., Segall, P., Kampes, B., 2004. A new method for measuring deformation on volcanoes and other natural terrains using InSAR Persistent Scatterers. *Geophysical Research Letters*, 31, L23611, doi: 10.1029/2004GL021737.

Kampes, B.M., Hanssen, R.F., 2004. Ambiguity Resolution for Permanent Scatterer Interferometry. *IEEE Transactions on Geoscience and Remote Sensing*, 42(11), pp. 2446-2453.

Lanari, R., Mora, O., Manunta, M., Mallorquí, J.J., Berardino, P., Sansosti, E., 2004. A small-baseline approach for investigating deformations on full-resolution differential SAR interferograms. *IEEE Transactions on Geosciences and Remote Sensing*, 42(7), pp. 1377-1386.

Mora O, Mallorquí JJ, Broquetas A (2003) Linear and nonlinear terrain deformation maps from a reduced set of interferometric SAR images. *IEEE Transactions on Geoscience and Remote Sensing* 41(10), pp. 2243-2253.

Pepe A, Sansosti E, Berardino P, Lanari R (2005) On the Generation of ERS/ENVISAT DInSAR Time-Series via the SBAS technique. *IEEE Transactions on Geoscience and Remote Sensing Letters*, 2, pp. 265–269.

Rosen PA, Hensley S, Joughin (2000) Synthetic Aperture Radar Interferometry. *Proc. of the IEEE*, 88 (3), pp. 333-382.